

# Analyst

Accepted Manuscript



This is an *Accepted Manuscript*, which has been through the Royal Society of Chemistry peer review process and has been accepted for publication.

*Accepted Manuscripts* are published online shortly after acceptance, before technical editing, formatting and proof reading. Using this free service, authors can make their results available to the community, in citable form, before we publish the edited article. We will replace this *Accepted Manuscript* with the edited and formatted *Advance Article* as soon as it is available.

You can find more information about *Accepted Manuscripts* in the [Information for Authors](#).

Please note that technical editing may introduce minor changes to the text and/or graphics, which may alter content. The journal's standard [Terms & Conditions](#) and the [Ethical guidelines](#) still apply. In no event shall the Royal Society of Chemistry be held responsible for any errors or omissions in this *Accepted Manuscript* or any consequences arising from the use of any information it contains.



## Analyst

## PAPER

## A TBET-based ratiometric probe for Au<sup>3+</sup> and its application in living cells†

Received 00th September 2015,  
Accepted 00th September 2015

Xiang Han,<sup>a</sup> Lei Zhao,<sup>b</sup> Dong-En Wang,<sup>a</sup> Juan Xu,<sup>a</sup> Longlong Zhang,<sup>a</sup> Mao-Sen Yuan,<sup>a</sup> Qin Tu<sup>a</sup> and Jinyi Wang<sup>\*ab</sup>

DOI: 10.1039/x0xx00000x

www.rsc.org/

In this paper, we designed and synthesized a novel TBET-based ratiometric fluorescent chemodosimeter RH-Au for Au<sup>3+</sup>. It was found that the probe RH-Au displayed highly selective, sensitive and naked-eye detection upon the addition of Au<sup>3+</sup>. The probe RH-Au can be used in a range of pH 6.0–7.5 and the detection limit was determined as low as 2.91 nM (0.57 ppb). We also demonstrated a successfully application of imaging Au<sup>3+</sup> in living cells by using RH-Au.

### Introduction

Gold ions emerged as special heavy metal ions have received great attentions in the past decades due to their versatile roles in chemistry and biology.<sup>1,2</sup> Gold ions are commonly used as mild and efficient catalysts for activating carbon-carbon multiple bonds.<sup>3</sup> And it is well known that gold ions possess anti-inflammatory properties and have been employed as valid agents in the treatment of many diseases such as arthritis, asthma and tuberculosis.<sup>4,5</sup> In addition, gold nanoparticles have been exploited as powerful platform for the application of biosensors, bio-imaging and drug delivery.<sup>6</sup> However, studies have demonstrated that gold ions may be highly toxic to the biological systems since they can strongly bind to DNA and proteins, and even cause the cleavage of DNA.<sup>7,8</sup> This may pose the great risk of these ions to human health and environment. Given the extensive usage of gold ions in the fields of chemistry, biology and medicine, the development of simple and sensitive methods for real-time monitoring of gold ions is highly desirable.

At present, analyses of trace metal ions usually rely on conventional techniques such as atomic absorption-emission spectrophotometry, inductively coupled plasma mass spectroscopy and electro-chemical analysis.<sup>9–11</sup> Despite the high sensitivity of these methods, it is difficult to use them for on-site and rapid detection due to the requirements of professional large-scale instruments and extensive pretreatment of samples. Alternatively, analyses of metal ions by fluorescence spectroscopy are much more convenient in terms of instrument operation, cost-effectiveness, and sample preparation.<sup>12</sup> The last

few decades have witnessed the flourishing development of fluorescent probes which are designed for the detection of various metal ion species in both environmental and biological samples.<sup>13–18</sup> Recently, some fluorescent probes have also been reported for monitoring gold ions with high sensitivity and selectivity.<sup>19–22</sup> However, most of these probes for gold ions are working in a single-fluorescent responsive manner, which is susceptible to environmental effects (such as pH, polarity and temperature). To avoid these limitations, ratiometric fluorescent probes for gold ions are highly demanded since they can measure the fluorescence intensities at two wavelengths and thus produce a built-in correction for environmental effects.<sup>23</sup> The excitation energy transfer (EET) is the most adopted methodology for addressing this issue. Two pathways are generally taken to realize the EET process. The first one is based on Förster resonance energy transfer (FRET). A FRET process needs the sufficient spectral overlap between the emission spectrum of energy donor and the absorption spectrum of energy acceptor. The donor and acceptor are usually linked by a non-conjugated spacer.<sup>24,25</sup> The other method is based on through-bond energy transfer (TBET). Different from FRET, in a TBET system, the donor and acceptor are linked via an electronically conjugated linker, which prevents the fragments of the donor and acceptor from becoming planar.<sup>26–27</sup> The energy transfer occurs through a bond, thus theoretically avoiding the limitation of spectral overlap. This feature endows the fluorescent probes based on TBET with high energy transfer efficiencies, fast energy transfer rates and large pseudo-stokes' shift. In recent years, some RH-based TBET probes have been reported for the detection of various metal ions.<sup>28–30</sup> However, to the best of our knowledge, probes based on TBET for gold ions have not yet been reported so far. Only two reports describe the design and synthesis of FRET-based fluorescent probes for gold ions.<sup>31,32</sup>

In this work, we designed and synthesized a novel TBET-based ratiometric fluorescent chemodosimeter **RH-Au** for Au<sup>3+</sup> with high selectivity and sensitivity. The probe **RH-Au**

<sup>a</sup> College of Science, Northwest A&F University, Yangling, Shaanxi 712100, P. R. China. Fax: +86-298-708-2520; Tel: +86-298-708-2520; Email: jywang@nwsuaf.edu.cn

<sup>b</sup> College of Veterinary Medicine, Northwest A&F University, Yangling, Shaanxi 712100, P. R. China.

† Electronic Supplementary Information (ESI) available. DFT calculation, Scheme S1, and Figs. S1–S26. See DOI: 10.1039/x0xx00000x

displayed a colorimetric change from colorless to pink and a ratiometric fluorescence transition from light green to red upon the addition of  $\text{Au}^{3+}$ . Moreover, a successful application of **RH-Au** for imaging  $\text{Au}^{3+}$  in living cells was also demonstrated.

## Experimental

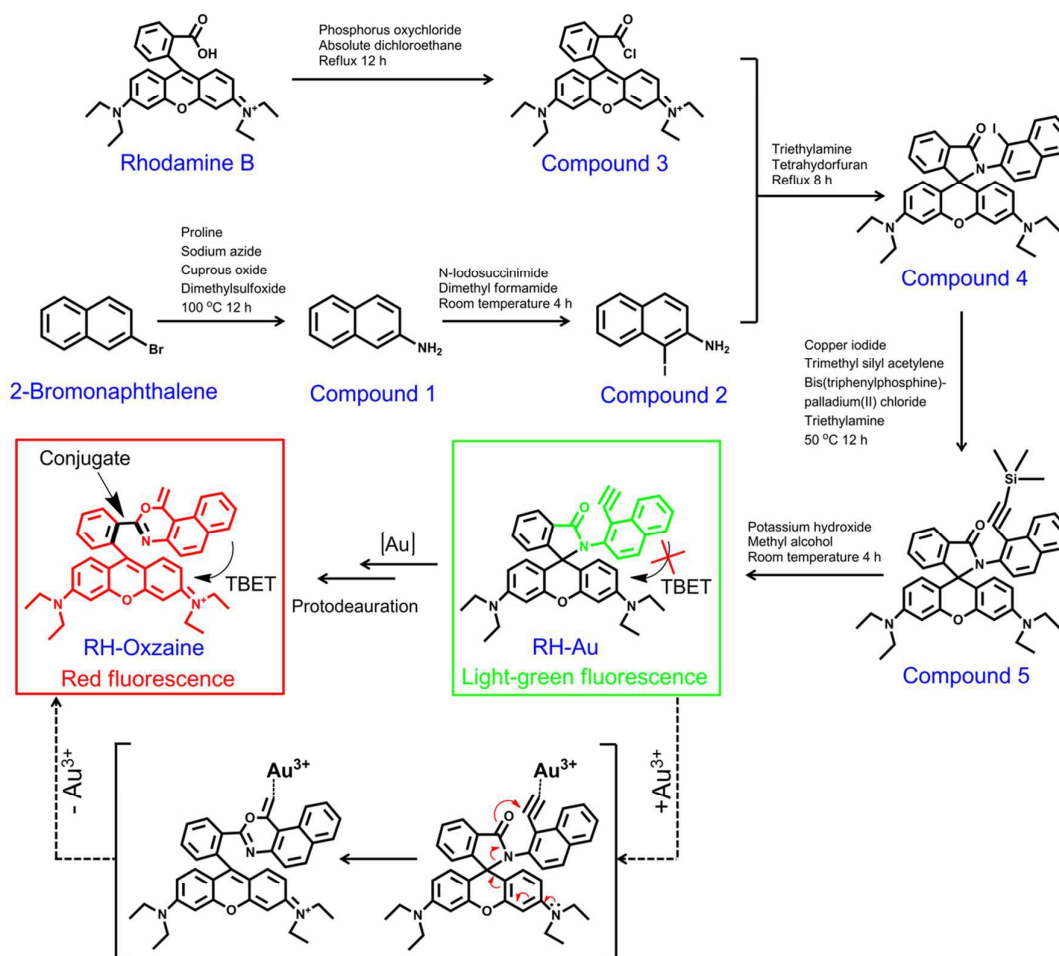
### Materials and apparatus

Rhodamine B was purchased from Alfa Aesar (Lancaster, England). 2-Bromonaphthalene, trimethyl silyl acetylene,  $\text{Cu}_2\text{O}$ ,  $\text{CuI}$ ,  $\text{NaN}_3$ , proline, phosphorus oxychloride, tetrakis (triphenylphosphine) palladium and N-Iodosuccinimide (NIS) were purchased from Aladdin (Shanghai, China). Dry solvents used in the synthesis were purified by using standard procedures. Human lung adenocarcinoma (A549) was obtained from the Chinese Academy of Sciences (Shanghai, China). All other reagents and solvents were of analytical grade and supplied by local commercial suppliers. Ultrapurified water was supplied by a Milli-Q system (Millipore®).

Reactions were monitored by thin-layer chromatography (TLC) using silica gel 60 GF254 (Qingdao Haiyang Chem. Co., Ltd., Shandong, China). Column chromatography was

conducted by using silica gel 60 (200–300 mesh; Qingdao Haiyang Chem. Co., Ltd.).  $^1\text{H}$ -nuclear magnetic resonance (NMR) and  $^{13}\text{C}$ -NMR spectra were recorded by using a BrukerAvance DMX 500 MHz/125 MHz spectrometer (Bruker, Billerica, MA, USA). Peaks were based on a tetramethylsilane (TMS) internal standard. Electrospray ionization mass spectroscopy (ESI-MS) data were obtained by using a Thermo Scientific LCQ FLEET mass spectrometer equipped with an electrospray ion source and controlled by Xcalibur software (Thermo Fisher Scientific, Waltham, MA, USA). UV-vis absorption spectra were recorded on a Shimadzu UV1800 spectrometer (Shimadzu, Kyoto, Japan). Fluorescence emission spectra were obtained on a Shimadzu RF-5301PC fluorescence spectrometer (Shimadzu). Imaging of A549 cells was performed under an inverted microscope (Olympus, CKX41) with a charge coupled device camera (Olympus, DP72) and a mercury lamp (Olympus, URFLT50). All pH measurements were performed with Model PHS-3C pH-meter (Shanghai, China). The absorbance was measured on a microplate reader (BioRad Model 680, USA) in the MTT assay.

### Synthesis



Scheme 1. The synthesis route and conditions for compound **RH-Au** and the possible mechanism of **RH-Au** for the detection of  $\text{Au}^{3+}$ .

SYNTHESIS OF COMPOUND **1**: Proline (150 mg, 1.3 mmol), NaN<sub>3</sub> (130 mg, 2 mmol), Cu<sub>2</sub>O (143 mg, 1 mmol) and 2-bromonaphthalene (207 mg, 1 mmol) were dissolved in DMSO after degassing under argon. The mixture was refluxed and stirred for 12 h. After cooling to room temperature, NH<sub>4</sub>Cl and ethyl acetate (20 mL) were added to the resultant solution and stirred for 1 h. Then, the mixture was filtered by Buchner funnel with fritted disc, and the organic layer washed with brine and water, dried over MgSO<sub>4</sub>. The crude product was purified by column chromatography on silica gel (ethyl acetate: petroleum ether = 10:1, v/v) to afford compound **1** (114.5 mg) as a brick-red solid with 80.1% yield. <sup>1</sup>H NMR (500 MHz, CDCl<sub>3</sub>) δ (ppm): 7.74-7.75 (d, 1H), 7.70-7.72 (d, 1H), 7.64-7.65 (d, 1H), 7.40-7.44 (t, 1H), 7.26-7.30 (t, 1H), 7.03-7.04 (d, 1H), 6.99-7.01 (m, 1H), 3.50-4.20 (b, 2H). <sup>13</sup>C NMR (125 MHz, CDCl<sub>3</sub>) δ (ppm): 144.13, 134.95, 129.24, 128.02, 127.75, 126.38, 125.83, 122.51, 118.27, 108.64.

SYNTHESIS OF COMPOUND **2**: NIS (300 mg, 1.3 mmol) was dissolved in anhydrous DMSO (15 mL) containing compound **1** (200 mg, 1.3 mmol). The resulting mixture was stirred for 6 h at room temperature. Subsequently, the solvent was removed under reduced pressure to obtain a black oily residue. The residue was purified by column chromatography on silica gel (ethyl acetate: petroleum ether = 10:1, v/v) to afford compound **2** (339 mg) as a black solid with 90.8% yield. <sup>1</sup>H NMR (500 MHz, CDCl<sub>3</sub>) δ (ppm): 8.07-8.09 (d, 1H), 7.73-7.75 (d, 1H), 7.59-7.61 (t, 1H), 7.37-7.40 (t, 1H), 6.98-6.99 (d, 1H), 4.31-4.40 (b, 2H). <sup>13</sup>C NMR (125 MHz, CDCl<sub>3</sub>) δ (ppm): 145.72, 135.66, 130.66, 130.55, 129.92, 128.57, 128.39, 128.26, 123.12, 117.01, 83.63.

SYNTHESIS OF COMPOUND **3**: Phosphorus oxychloride (225 mg, 0.45 mmol) was added to dichloromethane (30 mL) containing rhodamine B (450 mg, 1.01 mmol) under nitrogen. The resulting mixture was refluxed and stirred for 14 h. The solution was concentrated under vacuum to obtain compound **3** as an aubergine oily residue. The compound **3** was not purified and directly used to do the next reaction.

SYNTHESIS OF COMPOUND **4**: The compounds **2** (135 mg, 0.5 mmol) and **3** were dissolved in anhydrous tetrahydrofuran : triethylamine (100:1, v/v) solution. The resulting mixture was refluxed and stirred for 12 h. After cooling to room temperature, the solvent was removed under reduced pressure. The crude product was purified by column chromatography on silica gel (ethyl acetate : petroleum ether = 10:1, v/v) to afford compound **4** (260.7 mg) as a white solid with 75.1% yield. <sup>1</sup>H NMR (500 MHz, CDCl<sub>3</sub>) δ (ppm): 8.25-8.27 (d, 1H), 8.13-8.15 (d, 1H), 7.73-7.15 (d, 1H), 7.62-7.66 (m, 2H), 7.47-7.53 (m, 3H), 7.33-7.34 (dd, 1H), 6.91-6.92 (d, 1H), 6.71-6.72 (d, 1H), 6.46-6.48 (dd, 1H), 6.30-6.35 (m, 3H), 6.11-6.12 (d, 1H), 3.40-3.46 (dd, 4H), 3.27-3.31 (dd, 4H), 1.23-1.26 (t, 6H), 1.11-1.14 (t, 6H). <sup>13</sup>C NMR (125 MHz, CDCl<sub>3</sub>) δ (ppm): 165.89, 154.50, 153.74, 152.17, 149.07, 148.98, 132.84, 131.57, 129.01, 128.45, 127.87, 127.58, 126.90, 126.60, 126.37, 124.38, 108.42, 107.81, 107.38, 105.38, 98.02, 97.50, 66.67, 44.51, 44.33, 12.56.

SYNTHESIS OF COMPOUND **5**: The compound **4** (260 mg, 0.38 mmol), tetrakis (triphenylphosphine) palladium (8 mg, 0.01

mmol), CuI (3 mg, 0.01 mmol) were dissolved in anhydrous triethylamine : tetrahydrofuran (5:1, v/v). The mixture was stirred for 10 min, The trimethyl silyl acetylene (30 μL, 0.55 mmol) was added to the mixture. The resulting mixture was stirred for 12 h at 50 °C. After cooling to room temperature, the solution was concentrated under vacuum to obtain compound **5** as an orange oily residue. The compound **5** was not purified and directly used to do the next reaction.

SYNTHESIS OF COMPOUND **RH-Au**: The compound **5** was dissolved in anhydrous methanol containing KOH (10 mg) at room temperature. The resulting mixture was stirred for 6 h. The solvent was removed under reduced pressure. The crude product was purified by column chromatography on silica gel (ethyl acetate : petroleum ether = 5:1, v/v) to afford **RH-Au** (200 mg) as a yellow solid with 90.8% yield. <sup>1</sup>H NMR (500 MHz, CDCl<sub>3</sub>) δ (ppm): 8.32-8.33 (d, 1H), 8.12-8.13 (d, 1H), 7.73-7.74 (d, 1H), 7.56-7.59 (m, 3H), 7.45-7.53 (m, 2H), 7.25-7.26 (d, 1H), 6.78-6.91 (d, 2H), 6.43-6.45 (m, 3H), 6.37-7.38 (s, 1H), 6.25-6.26 (s, 1H), 6.11-6.12 (s, 1H), 3.54-3.44 (s, 1H), 3.27-3.43 (d, 8H), 1.11-1.25 (d, 12H). <sup>13</sup>C NMR (125 MHz, CDCl<sub>3</sub>) δ (ppm): 166.44, 153.19, 148.59, 134.17, 132.78, 132.02, 129.02, 128.20, 127.83, 126.86, 126.61, 126.30, 124.68, 124.18, 123.58, 108.53, 107.56, 105.21, 103.95, 97.97, 97.37, 86.62, 79.83, 68.39, 44.31, 12.59. ESI-MS m/z: calculated 691.29, found [M+H<sup>+</sup>], 692.54.

#### UV-Vis absorption and fluorescence measurements.

Stock solutions (0.1 M) of metal ions in water were prepared from KCl, NaCl, H<sub>2</sub>PtCl<sub>6</sub>·6H<sub>2</sub>O, HAuCl<sub>4</sub>·4H<sub>2</sub>O, CuSO<sub>4</sub>·5H<sub>2</sub>O, Zn(NO<sub>3</sub>)<sub>2</sub>·6H<sub>2</sub>O, CaCl<sub>2</sub>·2H<sub>2</sub>O, Ni(NO<sub>3</sub>)<sub>2</sub>·6H<sub>2</sub>O, HgCl<sub>2</sub>, MnSO<sub>4</sub>·H<sub>2</sub>O, Cd(NO<sub>3</sub>)<sub>2</sub>·4H<sub>2</sub>O, CoCl<sub>2</sub>·6H<sub>2</sub>O, FeCl<sub>2</sub>·4H<sub>2</sub>O, Al(NO<sub>3</sub>)<sub>3</sub>·9H<sub>2</sub>O, Fe(NO<sub>3</sub>)<sub>3</sub>·9H<sub>2</sub>O, CrCl<sub>3</sub>·6H<sub>2</sub>O, BaCl<sub>2</sub>·2H<sub>2</sub>O and AgNO<sub>3</sub>. **RH-Au** was exactly weighted and dissolved in acetonitrile to afford the probe stock solution (1 mM). For colorimetric and fluorescent detection of Au<sup>3+</sup>, the stock solution of **RH-Au** was diluted with 0.01M HEPES buffer (pH 7.4)/CH<sub>3</sub>CN (6:4, v/v) to obtain a 20 μM working solution. Then, different concentrations of Au<sup>3+</sup> were mixed with 3 mL of the working solution in a 1-cm cuvette. Unless otherwise stated, all the spectral studies were performed in 0.01M HEPES buffer (pH 7.4)/CH<sub>3</sub>CN (6:4, v/v) solution at room temperature. The fluorescence excitation wavelength was at 320 nm, with an emission wavelength range from 350 nm to 800 nm. Both the excitation and emission slit widths were 5 nm.

#### Cell culture and fluorescence imaging

The human lung adenocarcinoma (A549) cells were routinely cultured using Dulbecco's modified Eagle's medium (DMEM, Invitrogen, Grand Island, NY) supplemented with 10% FBS (Invitrogen), 100 units/mL penicillin, and 100 μg/mL streptomycin in a humidified atmosphere of 5% CO<sub>2</sub> at 37 °C. The cells were normally passaged at a ratio of 1:3 every three days to maintain their exponential growth phase. Before use, the cells were harvested through trypsinization with 0.25% trypsin (Invitrogen) in phosphate buffered solution (PBS, 0.01 M, pH 7.4) at 37 °C. Trypsinization was stopped upon the addition of fresh supplemented DMEM, and the cell suspension

was then centrifuged at 1000 rpm for 3 min. The cells were then resuspended in fresh DMEM for use. Afterward, the cells were seeded into 96-well microtiter plates ( $1.0 \times 10^4$  cells/well) with fresh medium (100  $\mu$ L). Subsequent incubation was permitted for 24 h before the cytotoxicity test. **RH-Au** (0–40.0  $\mu$ M/L) in 100  $\mu$ L of fresh medium was added to the respective test well. After 24 h incubation, MTT (10  $\mu$ L, 5 mg/mL) was added to each well. After 4 h, DMSO (100  $\mu$ L) was added to terminate the reaction. The absorbance was measured at 490 nm with a microplate reader. The cytotoxic effect of the probe was assessed by quantified the ratio of the absorbance of the probe treated cells versus the control cells.<sup>33</sup> All tests were performed in triplicate.

Prior to the imaging experiments, A549 cells were first washed thrice with PBS and incubated with 10  $\mu$ M **RH-Au** for 0.5 h at 37 °C. Then, they were incubated with 40  $\mu$ M  $\text{Au}^{3+}$  for another 0.5 h at 37 °C. Cell images before and after  $\text{Au}^{3+}$  treatment were taken in two channels, channel I,  $\lambda_{ex}$ : 460–490 nm and  $\lambda_{em}$ : 510–550 nm; channel II,  $\lambda_{ex}$ : 510–550 nm and  $\lambda_{em}$ : 570–620 nm.

## Results and discussion

### Synthesis of the probe **RH-Au**

The probe **RH-Au** was synthesized according to the synthetic route outlined in Scheme 1. The rhodamine-naphthylamine derivant **4** was directly obtained by coupling rhodamine B acid chloride with 1-iodo-2-naphthylamine in 75.1% yield. Trimethyl silyl acetylene was successfully introduced into compound **4** by Sonogashira reaction between terminal alkynyl and iodine in the presence of Pd ( $\text{PPh}_3$ )<sub>4</sub> and CuI as the catalyst to afford compound **5**. **RH-Au** was prepared by refluxing compound **5** and KOH in methanol for 6 h with a yield of 90.8%. The chemical structure of **RH-Au** was carefully characterized by <sup>1</sup>H NMR, <sup>13</sup>C NMR and ESI-MS. The detailed synthetic procedures and relevant spectral data are given in the experimental section and supplementary information (ESI†)

### The proposed sensing mechanism

In our newly designed probe for  $\text{Au}^{3+}$ , 1-alkynyl-2-naphthylamine derivant served as the energy donor and rhodamine B served as the energy acceptor were covalently linked through an amino bond (Scheme 1). The as-prepared probe **RH-Au** shows a light-green fluorescence emission resulting from the 1-alkynyl-2-naphthylamine moiety, and no fluorescence emission produced from the rhodamine B moiety due to the ring-closing of rhodamine B. Upon the addition of  $\text{Au}^{3+}$ , the probe **RH-Au** could convert to **RH-Oxazine**, in which the rhodamine B moiety undergoes a gold ion-catalyzed consecutive spiroactam ring-opening reaction and forms oxazine derivant with the 1-alkynyl-2-naphthylamine fragment through intramolecular cyclization process and subsequent protodeauration. Consequently, the excited energy of the 1-alkynyl-2-naphthylamine donor is transferred to the rhodamine acceptor and a strong red fluorescence emission produces from the fully conjugated xanthene moiety. The fluorescence

emission transformation allows ratiometric detection of  $\text{Au}^{3+}$  with high sensitivity and selectivity.

To confirm the detection mechanism of the probe **RH-Au** for  $\text{Au}^{3+}$ , density functional theory (DFT) calculations for the probe were first carried out by employing the B3LYP exchange functional and 6-31G\* basis sets (Fig. 1a). When the spiro-cyclization is closed with rhodamine conjugated structure being broken, the calculated energy gap of **RH-Au** is large as 3.831 eV, the dihedral angle between the donor and acceptor is 72.30° and the minimum distance of donor and acceptor plane is 2.58827 Å. However, when it is opened with its conjugated structure being recovered, the gap is 2.370 eV, the dihedral is 84.84° and the minimum distance is 2.71550 Å. Such calculation demonstrates that the donor and the acceptor fragments are not coplanar, which is favorable for the occurrence of the TBET process.

The reaction mechanism of **RH-Au** with  $\text{Au}^{3+}$  was further investigated by using <sup>1</sup>H NMR and ESI-MS spectra. The <sup>1</sup>H NMR spectral changes of **RH-Au** over time after adding  $\text{Au}^{3+}$  was performed in CD<sub>3</sub>CN (Fig. 1b). The result indicated that the reaction of 1 equiv  $\text{Au}^{3+}$  with **RH-Au** for 15 min led to a dramatic chemical shift change of the acetylene proton, where

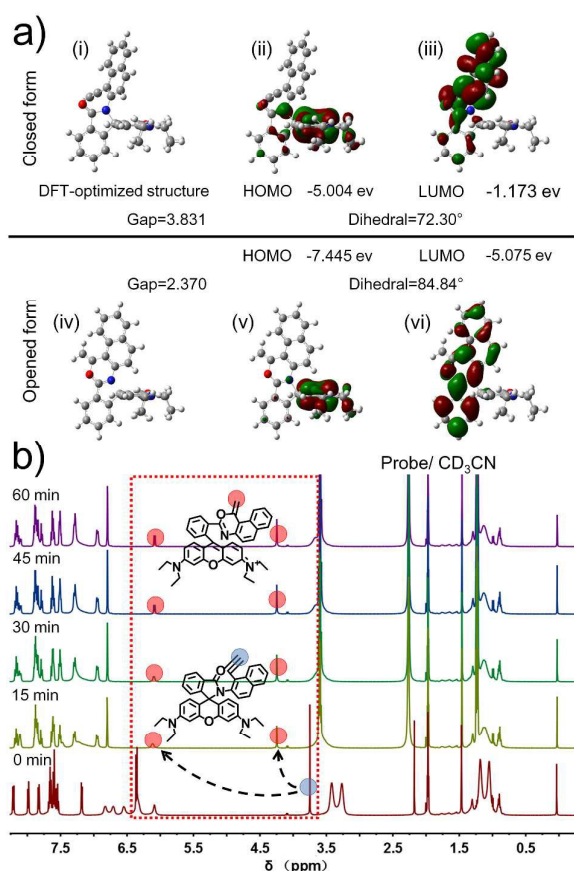


**Fig. 1** (a) Density functional optimized geometries of the closed and opened forms of **RH-Au**. (i and iv) DFT-optimized structure of **RH-Au** with the closed and opened forms. Molecular orbital plots HOMO (ii and v), LUMO (iii and vi), and HOMO/ LUMO energy gaps and dihedral of **RH-Au** in the closed or opened form. In the ball-and-stick representation, carbon, nitrogen and oxygen atoms are colored in gray, blue and red, respectively. H atoms are omitted for clarity. (b) The reaction between **RH-Au** (0.02 mM) and  $\text{HAuCl}_4$  (0.02 mM) in CD<sub>3</sub>CN was monitored by *in situ* NMR spectroscopy.

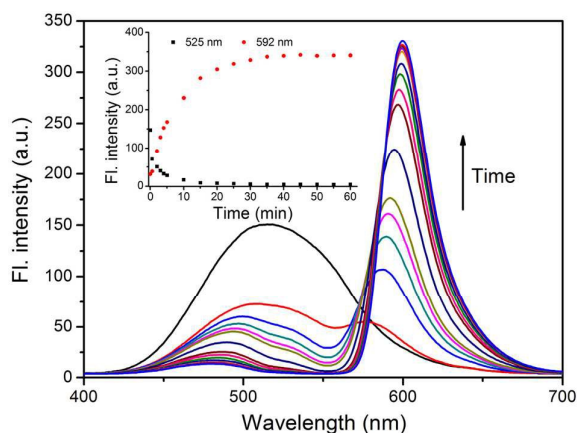


**Fig. 2** Time course of fluorescence change of **RH-Au** (20  $\mu\text{M}$ ) toward  $\text{Au}^{3+}$  (20  $\mu\text{M}$ ). Inset: time-dependent fluorescence ratio ( $F_{592}/F_{525}$ ) of **RH-Au** with  $\text{Au}^{3+}$  in  $\text{CH}_3\text{CN}/\text{H}_2\text{O}$  (4/6, v/v) buffered with HEPES (pH 7.4, 10 mM).  $\lambda_{\text{ex}} = 320 \text{ nm}$ .

the peak of the acetylene proton at 3.75 ppm disappeared, accompanied by the generation of a new peak at 4.25 ppm and 6.08 ppm. This phenomenon strongly revealed that the probe **RH-Au** converted to oxazine derivant, in which a vinylic proton formed to show a characteristic peak at 4.25 ppm and 6.08 ppm. Moreover, with the time increasing, the intensity of this peak enhanced, suggesting the deep completion of the reaction. The converted oxazine derivant was also confirmed by its  $\text{M}^+$  base peak at 592.53 (Fig. S1, ESI $\dagger$ ) measured by ESI-MS.

#### Fluorescence and absorption performance of **RH-Au** for $\text{Au}^{3+}$

To investigate the performance of the probe **RH-Au** for  $\text{Au}^{3+}$ , the absorption and fluorescence spectra of **RH-Au** (20  $\mu\text{M}$ ) with or without  $\text{Au}^{3+}$  were studied in HEPES buffer (10 mM, pH 7.4)/ $\text{CH}_3\text{CN}$  (6:4, v/v) solution. In the absence of  $\text{Au}^{3+}$ , only one absorption band could be observed at 325 nm, which should be ascribed to the absorption profile of 1-alkynyl-2-naphthylamine moiety (Fig. S2a, ESI $\dagger$ ). However, the absorption band was red-shift from 325 nm to 561 nm upon the addition of 5 equiv  $\text{Au}^{3+}$ , and the color of the solution concurrently changed from colorless to pink, suggesting the formation of the ring-open form of **RH-Au**. In addition, the excitation of the free **RH-Au** at 320 nm displayed a single emission band centered at 525 nm, which is attributed to the emission of the 1-alkynyl-2-naphthylamine moiety. The addition of  $\text{Au}^{3+}$  significantly decreased the fluorescence intensity around 525 nm, and simultaneously a new red-shifted emission band at around 592 nm gradually increased with the time increasing (Fig. S2b, ESI $\dagger$ ). The result clearly indicates that a TBET process occurred during the  $\text{Au}^{3+}$  catalyzed reaction of the probe **RH-Au**.

#### Sensitivity and selectivity of **RH-Au** for $\text{Au}^{3+}$ detection

A maximum fluorescence and absorption enhancement could be observed in less than 35 min after adding 5 equiv  $\text{Au}^{3+}$  (Fig. 2 and Fig. S3, ESI $\dagger$ ). The observed rate constant ( $k_{\text{obs}}$ ) of the reaction between the probe and  $\text{Au}^{3+}$  was determined as

$0.02372 \text{ min}^{-1}$  under the pseudo-first-order conditions (Fig. S4, ESI $\dagger$ ), which is comparable with the previous reported probes for gold ions.

To estimate the energy transfer efficiency (ETE) of **RH-Au** for  $\text{Au}^{3+}$ , the donor denoted as **JL-3** was also synthesized (Scheme S1, ESI $\dagger$ ). After the addition of  $\text{Au}^{3+}$ , **JL-3** showed a strong fluorescence emission centralized at 400 nm and there were no changes in the fluorescence intensity (Fig. S5, ESI $\dagger$ ). The results indicate that  $\text{Au}^{3+}$  has no effect on the fluorescence emission of **JL-3**, and thus ensure the occurrence of the TBET process between the donor and acceptor. The ETE of **RH-Au** for  $\text{Au}^{3+}$  was calculated to be 97.73% by Figs. S2 and S5 (ESI $\dagger$ ). Previous study has demonstrated that the TBET system was sometimes accompanied by FRET, resulting in the failure of energy transfer efficiency to reach 100%.<sup>30</sup>

The fluorescence titration of the probe **RH-Au** for  $\text{Au}^{3+}$  was performed in HEPES buffer (10 mM, pH 7.4)/ $\text{CH}_3\text{CN}$  (6:4, v/v) solution. Different concentrations of  $\text{Au}^{3+}$  were mixed with the probe solution (20  $\mu\text{M}$ ) respectively for 40 min and the fluorescence intensities of each solution were then measured (Fig. 3a), with the addition of  $\text{Au}^{3+}$  increasing, the donor's characteristic emission peak (525 nm) gradually decreased, while the characteristic emission peak (592 nm) of rhodamine

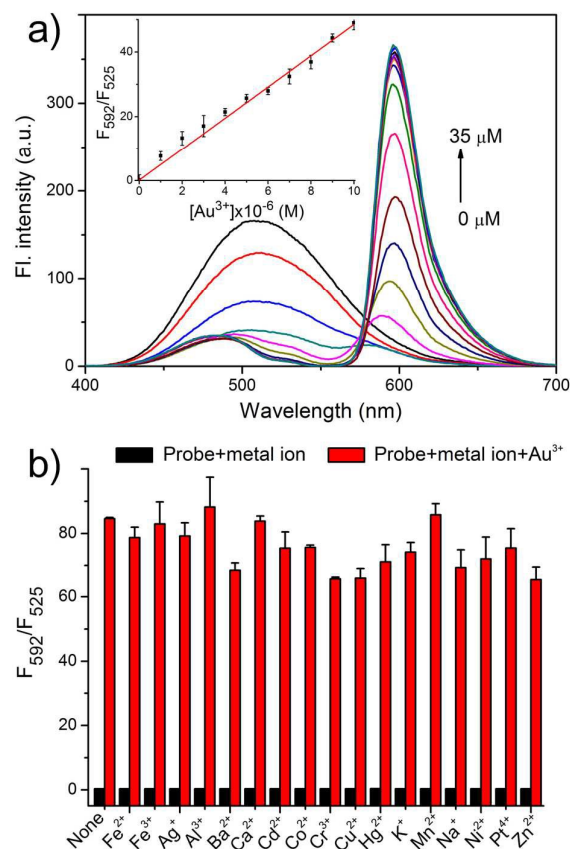


**Fig. 3** (a) Fluorescence spectra of **RH-Au** (20  $\mu\text{M}$ ) upon the addition of increasing amount of  $\text{Au}^{3+}$  (0-35  $\mu\text{M}$ ). Inset: the linear relationship of **RH-Au** between the fluorescence intensity and  $\text{Au}^{3+}$  concentration. (b) Fluorescence responses of **RH-Au** (20  $\mu\text{M}$ ) upon the addition of various metal ions (100  $\mu\text{M}$ ) (black column), and upon subsequent addition of  $\text{Au}^{3+}$  (red column).

B grew rapidly. The ratio of the fluorescence emission intensity between 592 nm and 525 nm displayed a good linear regression relationship ( $R^2 = 0.995$ ) with the concentration of  $\text{Au}^{3+}$  in the range of 1 to 10  $\mu\text{M}$  based on the titration experiment (Figs. 3a and S6, ESI†). The detection limit ( $3\sigma/\text{slope}$ ) was estimated to be as low as 2.91 nM (0.57 ppb) for  $\text{Au}^{3+}$ , which is lower or comparable than those fluorescent probes reported previously.<sup>29</sup> We also studied the fluorescence change with the concentration of  $\text{Au}^{3+}$  in the range of 0 to 1  $\mu\text{M}$ . A linear regression relationship ( $R^2 = 0.968$ ) was shown in Fig. S7 of the ESI†. This detection limit is sufficiently low for the detection of the submillimolar concentration of  $\text{Au}^{3+}$  found in many chemical and biological systems.

The selectivity of **RH-Au** for  $\text{Au}^{3+}$  over other metal ions was examined by UV-visible absorption and fluorescence emission spectra. Only the addition of  $\text{Au}^{3+}$  can cause a large as 22.9-fold increase in absorption band at 561 nm and a 259.77-fold increase in the ratio of fluorescence emission intensity between 592 nm and 525 nm (Figs. S8 and S9, ESI†). Other metal ions, such as  $\text{Fe}^{2+}$ ,  $\text{Fe}^{3+}$ ,  $\text{Ag}^+$ ,  $\text{Al}^{3+}$ ,  $\text{Ba}^{2+}$ ,  $\text{Ca}^{2+}$ ,  $\text{Cd}^{2+}$ ,  $\text{Co}^{2+}$ ,  $\text{Cr}^{3+}$ ,  $\text{Cu}^{2+}$ ,  $\text{K}^+$ ,  $\text{Mn}^{2+}$ ,  $\text{Na}^+$ ,  $\text{Ni}^{2+}$  and  $\text{Zn}^{2+}$  did exhibit negligible variations in absorption and emission spectra. The results indicate that the probe **RH-Au** displayed excellent selectivity for  $\text{Au}^{3+}$  toward other metal ions.

An interference experiment was further performed by adding  $\text{Au}^{3+}$  to the **RH-Au** solutions containing other metal ions (Fig. 3b). Before the addition of  $\text{Au}^{3+}$ , the ratios of fluorescence emission intensity between 592 nm and 525 nm were extremely low for each solution and no changes could be observed with the time increasing. However, when 5 equiv  $\text{Au}^{3+}$  were

introduced into the above solutions and incubated for 40 min, the ratios of fluorescence emission intensity between 592 nm and 525 nm were remarkable increased again. The results suggest that **RH-Au** can selectively detect  $\text{Au}^{3+}$  without the interference of other competitive species.

#### Effect of pH value on RH-Au detection for $\text{Au}^{3+}$

We also investigated the pH effect on the sensing property of **RH-Au** for  $\text{Au}^{3+}$  (Fig. S10, ESI†). The result exhibited that the probe **RH-Au** could efficiently work in the pH range from 6.0–7.5. This result promotes us to explore the possibility of **RH-Au** for ratiometric imaging  $\text{Au}^{3+}$  in living cells, because the probe showed an excellent detective performance at physiological pH.

#### Bio-imaging of the probe RH-Au in living cells

To evaluate the imaging performance of **RH-Au** for  $\text{Au}^{3+}$  in living cells, A549 cells chosen as the model cell line were incubated with **RH-Au** (10  $\mu\text{M}$ ) at 37 °C for 30 min. The cells showed intense fluorescence in the channel I and weak fluorescence in the channel II, corresponding to strong fluorescence at 525 nm and weak fluorescence at 592 nm. After treating the **RH-Au** cultured cells with 40  $\mu\text{M}$   $\text{Au}^{3+}$  for another 30 min at 37 °C, the fluorescent signal in the channel I decreased, while the fluorescence intensity in the channel II dramatically increased, suggesting the reaction of **RH-Au** with  $\text{Au}^{3+}$ , which caused the fluorescence signal conversion (Fig. 4 and Fig. S11, ESI†). The cytotoxicity experiment showed that the probe **RH-Au** was nearly nontoxic to live cells with its concentration less than 40.0  $\mu\text{M}$  (Fig. S12, ESI†). All the results suggest that **RH-Au** can be used as a ratiometric fluorescent probe to image  $\text{Au}^{3+}$  in living cells.

#### Conclusions

In summary, we have developed a new ratiometric fluorescent probe **RH-Au** based on TBET for the detection of  $\text{Au}^{3+}$ . This type of probe has such outstanding properties as high energy transfer efficiency, rapid response time, and high sensitivity and selectivity for  $\text{Au}^{3+}$ . In addition, **RH-Au** can be used as a ratiometric fluorescent probe for imaging  $\text{Au}^{3+}$  in A549 cells. We believe that this probe may provide an effective tool for studying significant gold ion related biological processes at the molecular level.

#### Acknowledgements

This work was supported by the National Natural Science Foundation of China (21175107 and 21375106) and the Fundamental Research Funds for the Central Universities (Z109021423).

#### Notes and references

- M. J. Jou, X. Q. Chen, K. M. K. Swamy, H. N. Kim, H. J. Kim, S. G. Lee and J. Y. Yoon, *Chem. Commun.*, 2009, 7218.
- H. Seo, M. E. Jun, O. A. Egorova, K. H. Lee, K. T. Kim and K. H. Ahn, *Org. Lett.*, 2012, **14**, 5062.

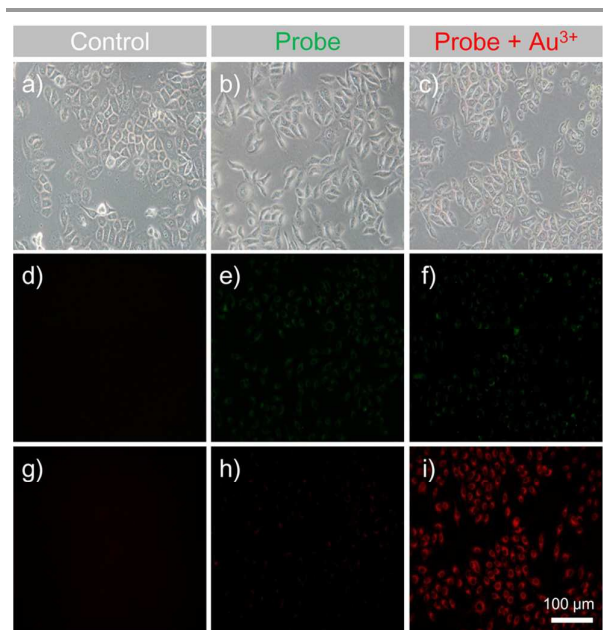


**Fig. 4** Fluorescent images of A549 cells treated with **RH-Au** (10  $\mu\text{M}$ ). (a) bright-field image of A549 cells incubated without **RH-Au**; (b) bright-field image of A549 cells incubated with **RH-Au** (10  $\mu\text{M}$ ) for 30 min; (c) bright-field image of A549 cells incubated with **RH-Au** (10  $\mu\text{M}$ ) for 30 min, followed by  $\text{HAuCl}_4$  (40  $\mu\text{M}$ ) for 30 min at 37 °C. Images observed through (d, e and f) channel I ( $\lambda_{\text{em}}$ : 510–550 nm) and (g, h and i) channel II ( $\lambda_{\text{em}}$ : 570–620 nm).

- 1  
2  
3  
4  
5  
6  
7  
8  
9  
10  
11  
12  
13  
14  
15  
16  
17  
18  
19  
20  
21  
22  
23  
24  
25  
26  
27  
28  
29  
30  
31  
32  
33  
34  
35  
36  
37  
38  
39  
40  
41  
42  
43  
44  
45  
46  
47  
48  
49  
50  
51  
52  
53  
54  
55  
56  
57  
58  
59  
60
- 3 J. H. Do, H. N. Kim, J. Y. Yoon, J. S. Kim and H. J. Kim, *Org. Lett.*, 2010, **12**, 932.
  - 4 J. Y. Choi, G. H. Kim, Z. Q. Guo, H. Y. Lee, K. Swamy, J. Y. Pai, S. H. Shin, I. Shin and J. Y. Yoon, *Biosens. Bioelectron.*, 2013, **49**, 438.
  - 5 J. B. Wang, Q. Q. Wu, Y. Z. Min, Y. Z. Liu and Q. H. Song, *Chem. Commun.*, 2012, **48**, 744.
  - 6 X. W. Cao, W. Y. Lin and Y. D. Ding, *Chem. Eur. J.*, 2011, **17**, 9066.
  - 7 A. Habib and M. Tabata, *J. Inorg. Biochem.*, 2004, **98**, 1696.
  - 8 E. E. Connor, J. Mwamuka, A. Gole, C. J. Murphy and M. D. Wyatt, *Small*, 2005, **1**, 325.
  - 9 A. Ohashi, H. Ito, C. Kanai, H. Imura and K. Ohashi, *Talanta*, 2005, **65**, 525.
  - 10 S. Lunvongsas, M. Oshima and S. Motomizu, *Talanta*, 2006, **68**, 969.
  - 11 A. Bobrowski, K. Nowak and J. Zarebski, *Anal. Bioanal. Chem.*, 2005, **382**, 1691.
  - 12 H. N. Kim, W. X. Ren, J. S. Kim and J. Yoon, *Chem. Soc. Rev.*, 2012, **41**, 3210.
  - 13 R. Z. Zhang and W. Chen, *Biosens. Bioelectron.*, 2014, **55**, 83.
  - 14 D. E. Kang, C. S. Lim, J. Y. Kim, E. S. Kim, H. J. Chun and B. R. Cho, *Anal. Chem.*, 2014, **86**, 5353.
  - 15 Y. Y. Han, C. Q. Ding, J. Zhou and Y. Tian, *Anal. Chem.*, 2015, **87**, 5333.
  - 16 H. J. Yin, B. C. Zhang, H. Z. Zhu, Y. Fan, M. Z. Zhu, G. X. Guo and X. M. Meng, *J. Org. Chem.*, 2015, **80**, 4306.
  - 17 U. R. G., F. Ali, N. Taye, S. Chattopadhyay and A. Das, *Chem. Commun.*, 2015, **51**, 3639.
  - 18 Z. Q. Guo, S. Park, J. Y. Yoon and I. J. Shin, *Chem. Soc. Rev.*, 2014, **43**, 16.
  - 19 E. Karakuş, M. Üçüncü and M. Emrullahoğlu, *Chem. Commun.*, 2014, **50**, 1119.
  - 20 Z. Öztaş, M. Pamuk and F. Algi, *Tetrahedron*, 2013, **69**, 2048.
  - 21 Y. T. Yang, C. X. Yin, F. J. Hou and J. B. Chao, *RSC Advances*, 2013, **3**, 9637.
  - 22 S. Kambam, B. H. Wang, F. Wang, Y. Wang, H. Y. Chen, J. Yin and X. Q. Chen, *Sensors and Actuators B*, 2015, **209**, 1005.
  - 23 M. H. Lee, J. S. Kim and J. L. Sessler, *Chem. Soc. Rev.*, 2015, **44**, 4185.
  - 24 A. P. de Silva, H. Q. N. Gunaratne, T. Gunnlaugsson, A. J. M. Huxley, C. P. McCoy, J. T. Rademacher and T. E. Rice, *Chem. Rev.*, 1997, **97**, 1515.
  - 25 J. S. Kim and D. T. Quang, *Chem. Rev.*, 2007, **107**, 3780.
  - 26 J. Fan, M. Hu, P. Zhan and X. Peng, *Chem. Soc. Rev.*, 2013, **42**, 29.
  - 27 J. C. T. Carlson, L. G. Meimetis, S. A. Hilderbrand and R. Weissleder, *Angew. Chem., Int. Ed.*, 2013, **52**, 6917.
  - 28 J. L. Fan, P. Zhan, M. M. Hu, W. Sun, J. Z. Tang, J. Y. Wang, S. G. Sun, F. L. Song and X. J. Peng, *Org. Lett.*, 2013, **15**, 492.
  - 29 Y. J. Gong, X. B. Zhang, C. C. Zhang, A. L. Luo, T. Fu, W. H. Tan, G. L. Shen and R. Q. Yu, *Anal. Chem.*, 2012, **84**, 10777.
  - 30 L. Y. Zhou, X. B. Zhang, Q. Q. Wang, Y. F. Lv, G. J. Mao, A. L. Luo, Y. X. Wu, Y. Wu, J. Zhang and W. H. Tan, *J. Am. Chem. Soc.* 2014, **136**, 9838.
  - 31 H. Seo, M. E. Jun, K. Ranganathan, K. H. Lee, K. T. Kim, W. Lim, Y. M. Rhee and K. H. Ahn, *Org. Lett.*, 2014, **16**, 1374.
  - 32 X. W. Cao, W. Y. Lin and Y. D. Ding, *Chem. Eur. J.*, 2011, **17**, 9066.
  - 33 U. Schatzschneider, J. Niesel, I. Ott, R. Gust, H. Alborzina and S. Wölfel, *Chem. Med. Chem.*, 2008, **3**, 1104.